52nd IEEE Conference on Decision and Control
December 10-13, 2013. Florence, Italy

Robust Fault Tolerant Pitch Control of Wind Turbines

Vahid Rezaei* and Kathryn E. Johnson†

Abstract— **A controller designed for a nominal wind turbine model may not work in presence of either unmodeled dynamics or sensor or actuator faults. We propose a multiple model robust control strategy for turbine speed regulation and wind disturbance rejection in presence of faults in a turbine's pitch actuator. The fault is inspired by recent challenges in wind turbine fault-tolerant control and consists of changed actuator dynamics. The simulation results confirm that an appropriate design of a set of robust controllers together with a soft switching among them is a reliable method for fault-tolerant control in this scenario.**

I. Introduction

As a clean and fast-growing renewable energy source, wind energy and particularly wind turbines (WTs) continue to attract interest from researchers around the world. Different advanced control methods have been developed to control WTs for different objectives, e.g. maximum power point tracking or load reduction. Increasing the size and flexibility of WTs increases the need for advanced controllers to obtain more energy from the wind while minimizing maintenance costs. The controlled system involves the WT and a set of sensors and actuators and is subjected to different abnormalities in its components. Thus, controllers that incorporate a plant model must be robust to unmodeled dynamics of the turbine as well as to the effects of sensor and actuator malfunctions on the closed loop wind energy system.

In this paper, the 3-bladed controls advanced research turbine (CART3) is used as a case study in anticipation of future field tests. This 600 kW WT with rotor diameter of 40 m has been configured for advanced controls testing and is located at the National Wind Technology Center near Boulder, Colorado, USA. CART3 is equipped with a full set of instruments that gather meteorological data at different heights. Blade and tower load sensors, tower-top accelerometers, and drive shaft torque transducers gather load and response data. This extensive suite of sensors provides a great data set for research purposes and also enables field testing of novel control algorithms. Control algorithms and objectives are described for the 2- and 3-bladed CARTs in [1]-[4]. However, these algorithms generally lack guarantees that control will perform correctly in the case of abnormalities in components of the closed loop system. For example, the effect of CART2 modeling uncertainty is discussed in [1], which concludes that such uncertainty may lead to instability of the closed loop system. Because continued operation in the presence of faults is desirable, it is necessary to investigate fault tolerant control (FTC) techniques for WTs.

Despite the fact that FTC is widely used in other applications, there is a limited research for FTC of WTs (see e.g., [5] and [6]). Different faults and their importance and detection strategies for the CARTs are described in [7]. Most papers in this field describe fault detection and isolation (FDI) techniques (e.g., [8]-[11]) and are based on the first WT fault tolerant benchmark model paper [12]. In general FTC schemes are divided into two groups [13]: passive and active. Passive control uses different robust control methods and active control usually includes a FDI unit in addition to a suitable controller, where the FDI is used to determine the plant's status and send the required commands to the plant. A well-designed active FTC system can outperform a well-designed passive one.

In this paper, a multiple model control strategy inspired by [14]-[16] is used to design an active robust FTC. The main idea of the proposed method is to design a set of controllers together with a suitable mixing mechanism based on the measurement (or estimation) of a fault-index, thereby adjusting the control signal and eliminating the effects of unwanted faults in WTs. Usually the performance requirements force the designer to include many local controllers in the final design. To reduce the number of the local controllers, each local controller is designed using a robust control technique; then, mixing is used for smooth transition among different robust controllers. We use a second order model for the faulty pitch actuator borrowed from [17] to design and simulate the proposed FTC scheme.

The remainder of this paper is organized as follows. A description of the WT model and actuator faults is presented in Section II and the control strategy is described in Section III. Simulation results are given in Section IV. Finally, Section V provides conclusions and future research ideas.

II. Wind Turbine Model

According to standard wind turbine control research practice, the CART3 is simulated using the FAST code [18]. All degrees of freedom (DOF) except yaw are enabled to perform the simulation in Section IV. When all DOF are enabled, FAST provides a linearized model of the CART3 with 30 states to model the generator, drive train, blade 1st and 2nd flapwise modes for each of the blades, blade 1st edgewise mode for each of the blades, tower 1st and 2nd for-aft modes, and tower 1st and 2nd side-to-side modes. This high dimension linear model will lead to a very high order

* Vahid Rezaei is with the department of Electrical Engineering and Computer Science at Colorado School of Mines, 1610 Illinois St., Golden, CO 80401, USA. Email: vrezaei@mines.edu

† Kathryn E. Johnson is with the department of Electrical Engineering and Computer Science at Colorado School of Mines and a Joint Appointee at National Renewable Energy Laboratory's National Wind Technology Center, Golden, CO, USA. Email: kjohnson@mines.edu

978-1-4673-5716-6/13/$31.00 ©2013 IEEE

controller. Thus, for linearization, we only enable some of the DOF and use the MBC code [19] to find the following state space model of CART3 for controller synthesis:

$$\begin{cases} \dot{x} = Ax + B\beta + B_d u_d \\ y = Cx \end{cases} \quad (1)$$

where x is the state vector, which includes drive train rotational displacement, rotor 1st symmetric flapwise deflection, generator speed, drivetrain rotational velocity, and rotor 1st symmetric flapwise velocity. In this representation, the control input β is the collective blade pitch angle command, u_d is the hub height wind speed disturbance and y is the measured generator speed. $A \in \mathbb{R}^{5\times5}$, $B \in \mathbb{R}^{5\times1}$, $B_d \in \mathbb{R}^{5\times1}$ and $C \in \mathbb{R}^{1\times5}$ are the system matrices.

The model in (1) does not include the pitch actuator states; hence, we augment a 2nd order linear model of the pitch actuator [17] to the CART3's synthesis and simulation models. This pitch actuator model is given by

$$\beta = \frac{\omega_n^2}{s^2+2\xi\omega_n s+\omega_n^2} u, \quad (2)$$

where the damping ratio ξ and natural frequency ω_n of the actuator are given in Table 1 for no fault and faulty conditions [6]. As shown in Table 1, ξ and ω_n vary depending on the fault type. Step responses from the control command signal u to the actual pitch angle β for the different cases in Table 1 are given in Fig. 1. These responses show that the faulty actuator has a slower dynamic than the no fault model. Therefore, the controller should be robust with respect to variations in these parameters.

Table 1: Fault parameters for the second order actuator model of the turbine.

	Parameter Value	
Actuator condition	ξ	ω_n (rad/s)
No fault	0.6	11.11
High air content in the oil	0.45	5.73
Pump wear	0.75	7.27
Hydraulic leakage	0.9	3.42
Pressure drop (low pressure)	0.9	3.42

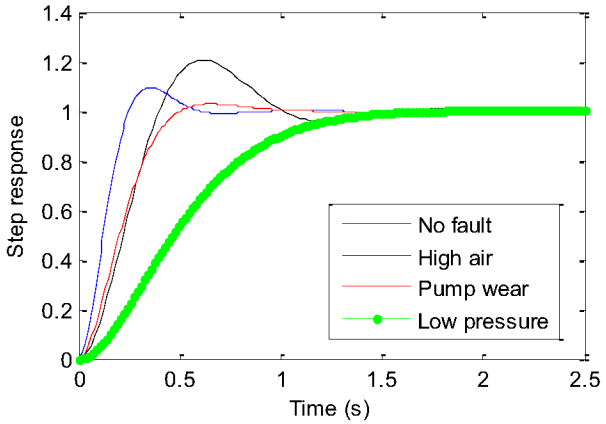

Fig. 1: Step responses of different actuator models given the parameters in Table 1

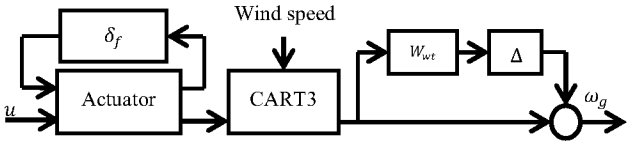

Fig. 2: Uncertain linear model of the augmented plant used to design the local robust controllers.

In robust control, we prefer to lump different uncertainties to have the fewest possible number of uncertain parameters, thus providing a less conservative design. Motivated by [5] and [6], if we combine the vertices of the parameters in Table **1** to have a convex approximation, then we can approximate the changes in ξ and ω_n to just one fault index θ_f by

$$\omega_n^2(\theta_f) = \omega_{n,0}^2 + (-\omega_{n,0}^2 + \omega_{n,lp}^2)\theta_f, \quad (3)$$

$$\xi\omega_n(\theta_f) = \xi_0\omega_{n,0} + (-\xi_0\omega_{n,0} + \xi_{n,lp}\omega_{n,lp})\theta_f, \quad (4)$$

where ξ_0 and $\omega_{n,0}$ are the damping ratio and natural frequency the actuator model with no fault, $\xi_{n,lp}$ and $\omega_{n,lp}$ are the parameters of the actuator with low pressure fault, and $\theta_f \in [0,1]$. Then, $\theta_f = \bar{\theta}_f(1 + p_f\delta_f)$ will be used for robust control design, where $\bar{\theta}_f$ is the nominal fault index, θ_f is the uncertain fault index, p_f is the uncertainty weight and $|\delta_f| \le 1$ is the real-valued uncertainty. Fig. 2 shows the block diagram of the augmented actuator-WT model for robust control design purpose where ω_g is the measured generator speed, W_{wt} is a weighting function, and $|\Delta| \le 1$ is the complex-valued uncertainty. It should be noted that the "nominal" model is obtained for the case that $\theta_f = \bar{\theta}_f$ when $p_f = 0$, which is different from the "no fault" model, where $\theta_f = 0$.

III. FTC Synthesis

In this section, we introduce the robust fault tolerant pitch controller that is designed based on multiple model robust control strategy. Such a control system makes it possible to have the advantages of both active and passive FTC as mentioned in [13]. The general idea is to use the fault index θ_f to find different intervals and design a local robust controller for each interval. Then, a mixing approach is implemented to determine the control signal u that is sent to the actuator.

A. FTC design procedure

The design procedure for robust fault tolerant pitch control is as follows (restated for FTC design from [14]):

1. Find the LTI model of the WT, choose an acceptable order for the model, and call this it the "nominal model." Then, augment the nominal model with the actuator model (2) with the parameters as defined in (3) and (4).
2. Assume θ_f is the uncertain varying parameter in the nominal model that changes from $\theta_{f,min} = 0$ for no fault to $\theta_{f,max} = 1$ for low pressure cases.
3. Determine a robust synthesis configuration for the FTC problem (see III.B). As a guideline for determining a performance index used to select the number of required

models, consider the wind speed disturbance to be an unwanted external input. Its effect on regulated speed should be as small as possible for all actuator conditions. Here, this performance criterion is based on disturbance rejection properties of the fault tolerant pitch controller. In other words, this configuration makes it possible to define a performance criterion C_f that can be used to determine the length of each local θ_f interval (uncertain parameter), systematically (steps 4-5).

4. First, we must determine the upper limit on the design; that is, the best possible performance.
   4.1. start with the LTI model for the case that $\theta_f = \theta_{f,min}$. Design a robust controller with acceptable stability and performance (in our design, this is determined based on $peak - \mu$ values; see III.B). Then, name the corresponding C_f as C_f^{1*} where "1" stands for the number of the local FTC and * means there is no uncertainty in θ_f.
   4.2. Determine an acceptable resolution ε_θ for the step size. Redo Step 4.1 for $\theta_\varepsilon^{i*} = \theta_{f,min} + i \times \varepsilon_\theta$ for $i = 1,2,\dots,N$ where N is determined based on the step size and $\theta_\varepsilon^{i*} \in [\theta_{f,min}, \theta_{f,max}]$ (for example, if $\varepsilon_\theta = 0.1$, then $N = 10$) If we call the resulting performance C_f^{i*}, then we will have a table of performance criterion C_f^{i*} versus θ_ε^{i*} as maximum achievable performance for each θ_ε^{i*}.
5. At this step, we have to design an acceptable number of robust controllers. Hence, we assume there is an uncertainty in θ_f and design a more realistic second set of controllers that will be implemented in simulation.
   5.1. To do this, in synthesis, we set $C_f^1 = kC_f^{1*}$ where $k \leq 1$ is a design parameter. Then, we increase the length of the first uncertain interval $[\theta_{f,min}, \theta_{f,1}]$ to synthesize a robust controller for this interval.
   5.2.Then, starting from $\theta_{f,1}$, we follow the same procedure up to the $\theta_{f,max}$.
   5.3. As the fault index goes from $\theta_{f,min}$to $\theta_{f,max}$, the control objective should change from maximum wind speed disturbance rejection to maximum lifetime for the actuator. Therefore, when moving to the next interval, decrease C_f^j for j^{th} local robust controller. As a result, the effect of the actuator weighting function W_u is increased in the design procedure such that in faulty cases the controller will use the actuator less than in the no fault case.
6. Finally, measure or estimate the uncertainty parameter θ_f to weight different controllers appropriately such that the overall FTC has good transient behavior from one local FTC to the next.

B. *Design of local robust fault tolerant pitch controllers*

Instead of other conventional robust controllers such as $\mathcal{H}_\infty$, we use the $mixed - \mu$ method to design the local FTCs because it provides a formulation to consider both robust stability and robust performance. The theory of the $mixed - \mu$ method is well discussed in the robust control literature (e.g., [20] and [21]) and is therefore not detailed in this paper.

The synthesis configuration that we use to design different local robust controllers is shown in Fig. 3, where an additional block M_{zh} is added to enable integral action in the robust controller [20]. In Fig. 4, it is clear that most of the wind speed's power is at low frequencies. Hence, we can treat the wind speed as a disturbance. The weights W_d and W_p are determined based on the frequency shape of the wind profiles. We use a constant W_u to weigh the actuation signal equally over the entire frequency range. $W_T$is designed iteratively in simulation to have an acceptable closed loop response.. Our resulting weighing functions are therefore.

$$W_d = C_d \frac{0.3}{s+0.3},\ W_p = C_f C_P \frac{0.67s+3.3}{s^2+1.02s+0.02},$$
$$W_T = C_f C_T \frac{0.18s+0.67}{0.18s+1},\ W_u = C_u,$$
$$W_{wt} = C_{wt} \frac{0.17s+0.01}{0.01s+1},\ M_{zh} = \frac{s+\alpha}{s}.$$

where C_f is the performance criterion, and C_d, C_p, C_T, C_u and C_{wt} are constants. Also, α is an arbitrary positive number to provide the required integral action. This configuration produces the general structure for $mixed - \mu$ control design as shown in Fig. 5 where the block diagonal uncertainty matrix on the top is a combination of the real and complex uncertainties as mentioned in Section II. Also, $P(s)$ is the generalized plant that includes the actuator model, the CART3 model, and the weighting functions. Furthermore, $K(s)$ is the controller to be designed.

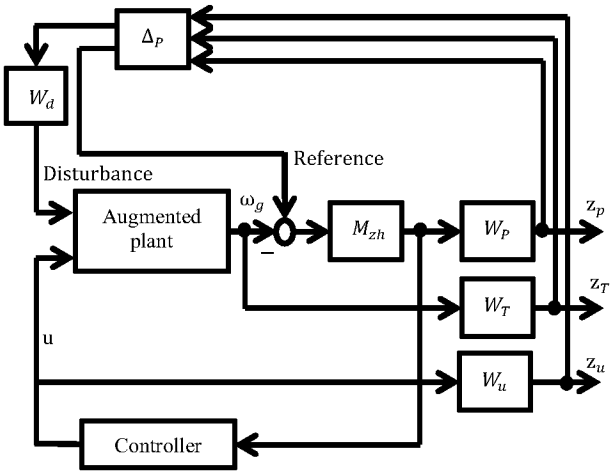

Fig. 3: Synthesis configuration for local FTC design

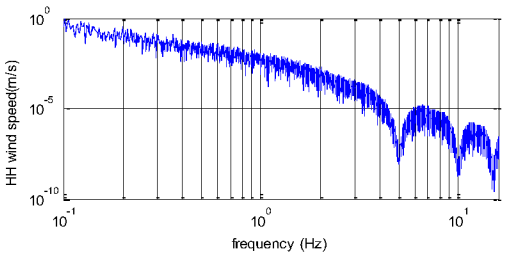

Fig. 4: Power spectral density of the used hub-height wind speed

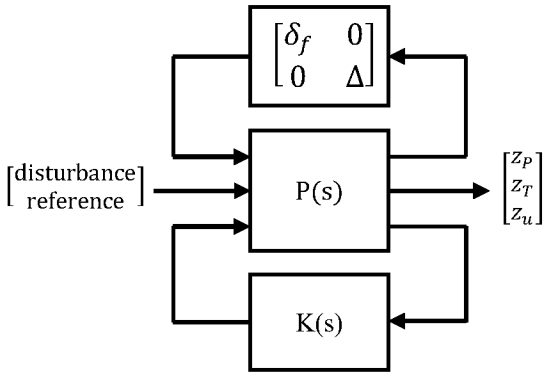

Fig. 5: General structure for $mixed-\mu$ problem

The results of some $mixed-\mu$ control designs for certain θ_fs are given in Table 2. In all cases, the $peak-\mu$ value is around 0.99 to ensure both stability and acceptable performance of the closed loop system. The local robust FTCs are summarized in Table 3. The lengths of the overlaps in the θ_f intervals are obtained by trial and error, but each interval's length is determined with the help of the $mixed-\mu$ design algorithm such that the $peak-\mu$s remain around 0.99 for all cases, again for closed-loop stability and performance.

The order of each local controller in Table 3 was originally designed to be 23, which is high and may therefore lead to the implementation issues. This high order is due to the effect of adding uncertainty in θ_f and still having guarantees for robust stability and robust performance. Therefore, we use order reduction techniques to reduce the order of all controllers to 8 or 9 as given in Table 3. Fig. 6 shows that the reduced order controller has a very similar frequency response as the full order.

Table 2: Maximum achievable C_f

θ_f^*	0.0	0.2	0.4	0.6	0.8	1.0
C_f^*	1	0.995	0.984	0.965	0.940	0.80

Table 3: Local robust FTCs

# of controller	θ_f	C_f	$peak-\mu$	Reduced order
1	[0.000,0.150]	0.700	0.987	9
2	[0.120,0.240]	0.696	0.988	9
3	[0.210,0.320]	0.696	0.989	9
4	[0.300,0.400]	0.696	0.988	9
5	[0.380,0.475]	0.688	0.989	9
6	[0.460,0.545]	0.686	0.986	9
7	[0.530,0.610]	0.680	0.991	9
8	[0.600,0.670]	0.675	0.984	8
9	[0.660,0.720]	0.675	0.976	8
10	[0.715,0.775]	0.664	0.994	8
11	[0.770,0.820]	0.660	0.984	8
12	[0.815,0.860]	0.651	0.982	8
13	[0.855,0.895]	0.645	0.981	8
14	[0.890,0.930]	0.630	0.998	8
15	[0.925,0.965]	0.568	0.995	8
16	[0.960,1.000]	0.546	0.994	8

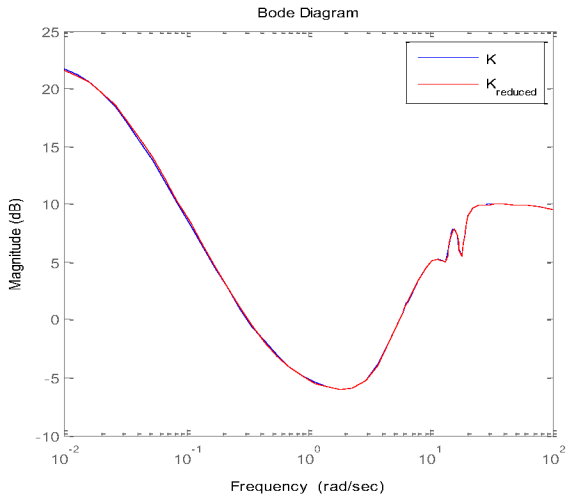

Fig. 6: Bode magnitude plot comparison of the full order and reducer order models for 16th controller

C. *Mixing the output of local controllers*

We use the mixing method introduced in [15] and [16] to continuously weigh the local controllers such that at each time no more than two controllers are effective independent of the number of the local controllers. Moreover, because of its continuity, this mixing method provides a bumpless transfer from one local FTC to another as the local FTCs are designed to be stable. To implement mixing, we parameterize the trapezoidal functions (5) for the 16 intervals given in Table 3 such that the final control signal is a weighted signal based on the local FTCs as given by (6).

$$T(x,a,b,c,d)=\begin{cases}0 & x<a \text{ or } x>d\\ \frac{x-a}{b-a} & a\le x\le b\\ 1 & b\le x\le c\\ \frac{d-x}{d-c} & c\le x\le d\end{cases} \quad (5)$$

$$u=\sum_{i=1}^{16}\frac{T_i(\theta_f,a_i,b_i,c_i,d_i)}{\sum_{j=1}^{16}T_j(\theta_f,a_j,b_j,c_j,d_j)}u_i \quad (6)$$

where a, b, c, and d are design parameters that determine the shape of the mixing functions for each of the local intervals. For example, the 3rd mixing function is T(θ_f,0.21,0.24,0.30,0.32). The block diagram of the closed loop system is shown in Fig. 7, where u is the control signal and CM stands for the condition monitoring software, which gives the estimation of the fault index. Our industry partner, Michigan Aerospace Corporation, has proprietary CM software that enables us to assume the estimated fault index is equal to the actual one.

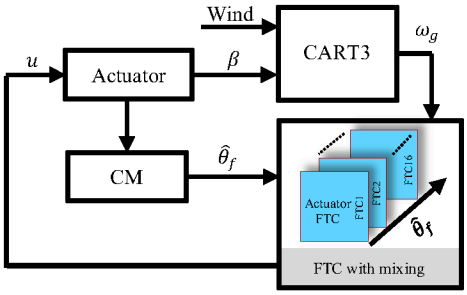

Fig. 7: Closed loop wind energy conversion system with FTC

IV. Simulation Results

In this section, we implement the FTC with mixing to control the nonlinear model of CART3 augmented with a second order pitch actuator [17] as shown in Fig. 7. To perform the simulations, we use a full non-linear CART3 model within the U.S. National Renewable Energy Laboratory's FAST code. The control objective is to regulate the generator speed, which is a measured signal, to its rated value of 1800 rpm in the presence of the wind disturbance and in spite of faults in pitch actuator. This regulation is accomplished by collectively pitching the blades while the pitch actuator signals never exceed their limits. For CART3, the pitch angle, rate and acceleration should stay within [0, 20] deg, [-18, 18] deg/s, and [-150, 150] deg/s^2 for normal operation, respectively [22]. However, we have limited the pitch rate to 3 deg/s in our simulation for increased robustness.

Fig. 8 shows the simulation results of FTC with mixing. The top subplot shows the hub-height wind speed, which is within region 3. This wind input has a mean speed equal to 18 m/s and 12.20% turbulence intensity. The fault scenario is shown in the second subplot, where $\theta_f = 0$ means there is no fault and $\theta_f = 1$ stands for low pressure in the pitch actuator (see Table 1). The third subplot depicts the number of the controller that is active at each time. Note that on a boundary around the step times, the mixing approach keeps two adjacent local controllers active, which is not shown in Fig. 8. The bottom subplot confirms that the proposed controller is able to regulate the generator speed around its rated value in spite of the faulty actuator. Moreover, the regulation performance is similar for the faulty and no fault cases. Also, bumpless transfer enabled by mixing is apparent since there are no transient spikes in the controlled signal.

Fig. 9 shows the pitch actuation signals for the faults in actuator and proposed FTC method. As is clearly visible in the pitch acceleration signal, during the fault (200-275 s) the FTC uses the actuator less than when there is no fault (50-100 s and 375-450 s) as it tries to keep the turbine operating. In all of the signals, even the pitch acceleration, there is no transient spike when changing the local controllers. Moreover, all signals are within their allowable limits.

Although the proposed FTC provides no guarantee on component loads, Fig. 10 and Fig. 11 show that the controller causes no unusual loads on turbine components during the fault times.

V. Conclusion and Future Work

In this paper, a multiple model robust controller with mixing based on the measurement of the fault index is proposed for pitch actuator faults given in a WT fault tolerant control challenge. The multiple controllers are designed based on the $mixed-\mu$ approach such that for each local interval of the fault index, there are guarantees for both robust stability and robust performance.

The next step is to design a multiple model–multiple parameter controller for both fault index and wind speed changes to further improve the dynamic response of the closed loop system with respect to the wind disturbance using a LIDAR sensor provided by an industrial partner.

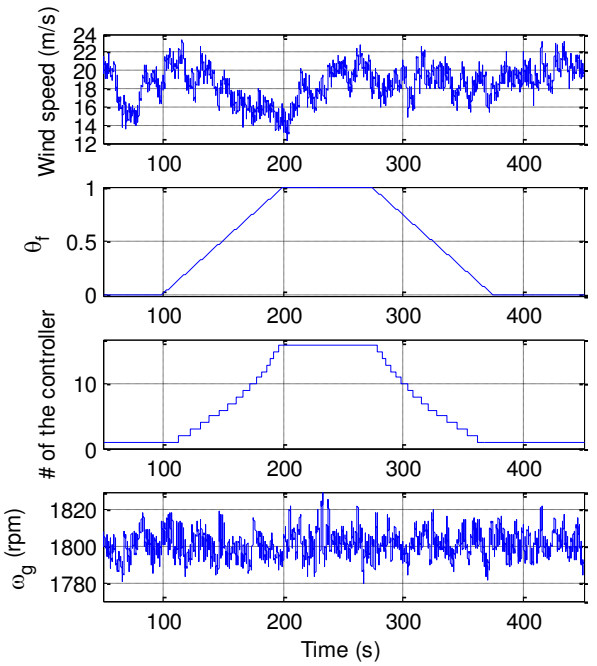

Fig. 8: Simulation results of FTC with mixing

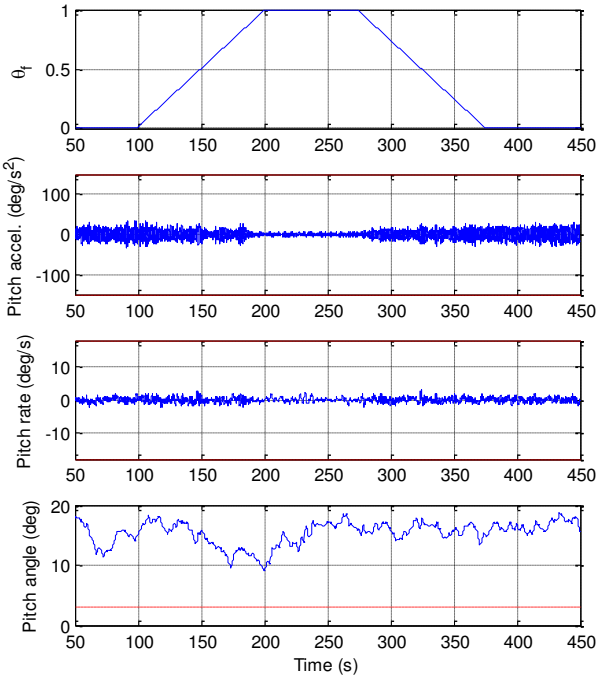

Fig. 9: Actuator signals

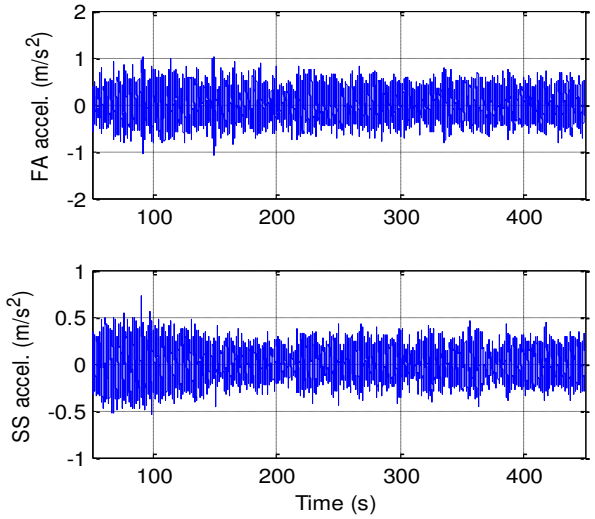

Fig. 10: Tower fore-aft acceleration (top) and tower side-to-side acceleration (bottom) for the given fault scenario.

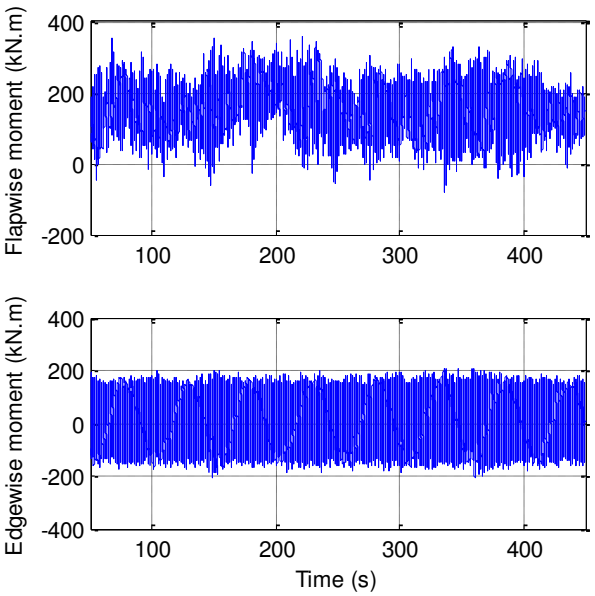

Fig. 11: Blade 1 moments for the given fault scenario.

REFERENCES

[1] Wright A. D., *Modern Control Design for Flexible Wind Turbines,* National Renewable Energy Lab., Golden, CO, NREL/TP-500-35816, July 2004.

[2] Wright A. D., Fingersh L. J., *Advanced control design for wind turbines; Part I: control design, implementation, and initial tests*, National Renewable Energy Lab., Golden, CO, NREL/TP-500-42437, March 2008.

[3] Laks J. H., Pao L. Y., Wright A. D.; "Control of Wind Turbines: Past, Present, and Future," *American Control Conference*, St. Louis, MO, pp. 2096-2103, June 2009.

[4] Fleming P. A., Wingerden J. V., Wright A. D., "Comparing State-Space Multivariable Controls to Multi-SISO Controls for Load Reduction of Drivetrain-Coupled Modes on Wind Turbines through Field-Testing," *50th AIAA Aerospace Sciences Meeting including the New Horizons Forum and Aerospace Exposition*, January 2012.

[5] Sloth C., Esbensen T., Stoustrup J., "Robust and fault-tolerant linear parameter-varying control of wind turbines," *Mechatronics*, Vol. 21, Issue 4, pp. 645-659, 2011.

[6] Adegas F. D., Sloth C., Stoustrup J., *Control of Linear Parameter Varying Systems with Applications*, Springer-Verlag Berlin Heidelberg, pp.303-337, 2012.

[7] Johnson K. E., Fleming P. A., "Development, implementation, and testing of fault detection and condition monitoring on the national wind technology center's controls advanced research turbines," *Mechatronics*, Vol. 21, Issue 4, pp. 728–736, 2011.

[8] Chen W., Ding S. X., Haghani A., Naik A., Khan A. Q., Yin S., "Observer-based FDI Schemes for Wind Turbine Benchmark," *18th IFAC World Congress,* Milano (Italy), pp. 7073-7078, 2011.

[9] Negre P., Puig V., Pineda I., "Fault Detection and Isolation of a Real Wind Turbine using LPV Observers," *18th IFAC World Congress,* Milano (Italy), pp. 12372-12379, 2011.

[10] Pisu P., Ayalew B., "Robust Fault Diagnosis for a Horizontal Axis Wind Turbine", *18th IFAC World Congress,* Milano (Italy), pp. 12372-12379, 2011.

[11] Svard C., Nyberg M., "Automated Design of an FDI-System for the Wind Turbine Benchmark," *18th IFAC World Congress,* Milano (Italy), pp. 8307-8315, 2011.

[12] Odgaard P. F. , Stoustrup J., Kinnaert M., "Fault Tolerant Control of Wind Turbines a benchmark model," *Proc. IFAC Symp. on Fault Detection Supervision and Safety for Technical Processes,* (Spain), pp. 155-160, 2009.

[13] Jiang J., Yu X., "Fault-tolerant control systems: A comparative study between active and passive approaches," *Annual Reviews in Control*, Vol. 36, Issue 1, pp. 60–72, 2012.

[14] Fekri S., Athans M., Pascoal A., "Issues, progress and new results in robust adaptive control," *Int. J. Adaptive Control and Signal Processing*, vol. 20, no. 10, pp. 519–579, 2006.

[15] Kuipers M., Ioannou P. A., "Practical Robust Adaptive Control: Benchmark Example," *American Control Conf.*, pp.5168-5173, June 2008.

[16] Kuipers M., Ioannou P. A., "Multiple Model Adaptive Control with Mixing," *IEEE Trans. Automatic Control*, pp.1822-1836, 2010.

[17] Odgaard P. F., Johnson K. E., "Wind turbine fault detection and fault tolerant control - a second challenge," *American Control Conf.*, 2013.

[18] Jonkman J. M., Buhl M. L., *FAST user's guide,* National Renewable Energy Lab., Golden, CO, NREL/EL-500-38233, August 2005.

[19] Bir G. S., *User's Guide to MBC3: Multi-Blade Coordinate Transformation Code for 3-Bladed Wind Turbines,* National Renewable Energy Lab., Golden, CO, NREL/TP-500-44327, September 2010.

[20] Zhou K., Doyle J., *Essentials of Robust Control,* Prentice Hall, 1997.

[21] Skogestad S., Postlethwaite I., "Multivariable Feedback Control Analysis and Design," 2nd ed, *John Wiley & Sons*, 2001.

[22] Fingersh L. J., Johnson K. E., *Baseline Results and Future Plans for the NREL Controls Advanced Research Turbine*, National Renewable Energy Lab., Golden, CO, NREL/CP-500-35058, November 2003.